

CORRECTIONS

CHEMISTRY, BIOPHYSICS AND COMPUTATIONAL BIOLOGY

Correction for “Probing the relative orientation of molecules bound to DNA through controlled interference using second-harmonic generation,” by Benjamin Doughty, Yi Rao, Samuel W. Kazer, Sheldon J. J. Kwok, Nicholas J. Turro, and Kenneth B. Eisenthal, which appeared in issue 15, April 9, 2013, of *Proc Natl Acad Sci USA* (110:5756–5758; first published March 25, 2013; 10.1073/pnas.1302554110).

The authors note that the following statement should be added to the Acknowledgments: “We also acknowledge funding from the Chemical Sciences, Geosciences and Bioscience Division, Office of Basic Energy Sciences, Office of Science of the US Department of Energy.”

www.pnas.org/cgi/doi/10.1073/pnas.1310422110

IN THIS ISSUE

Correction for “In This Issue,” which appeared in issue 21, May 21, 2013, of *Proc Natl Acad Sci USA* (110:8315–8316; 10.1073/iti2113110).

The authors note that within “Measuring telomeres in single cells” on page 8316 the writing credit “C.R.” should instead appear as “C.B.” The online version has been corrected.

www.pnas.org/cgi/doi/10.1073/pnas.1310833110

NEUROSCIENCE

Correction for “Progressive dopaminergic cell loss with unilateral-to-bilateral progression in a genetic model of Parkinson disease,” by Maxime W. C. Rousseaux, Paul C. Marcogliese, Dianbo Qu, Sarah J. Hewitt, Sarah Seang, Raymond H. Kim, Ruth S. Slack, Michael G. Schlossmacher, Diane C. Lagace, Tak W. Mak, and David S. Park, which appeared in issue 39, September 25, 2012, of *Proc Natl Acad Sci USA* (109:15918–15923; first published September 10, 2012; 10.1073/pnas.1205102109).

The authors note that the incorrect term appeared for the mice background that they used. All instances of “C57BL/6J” should instead appear as “C57BL/6.” The locations were:

On page 15918, left column, line 4 within the Abstract

On page 15918, right column, first full paragraph, line 5

On page 15922, left column, second full paragraph, line 2

These errors do not affect the conclusions of the article.

www.pnas.org/cgi/doi/10.1073/pnas.1310560110

Quantitative field theory of the glass transition

Silvio Franz^a, Hugo Jacquin^b, Giorgio Parisi^{c,d,1}, Pierfrancesco Urbani^{a,d}, and Francesco Zamponi^e

^aLaboratoire de Physique Théorique et Modèles Statistiques, Centre National de la Recherche Scientifique et Université Paris-Sud 11, Unité Mixte de Recherche 8626, 91405 Orsay Cedex, France; ^bLaboratoire Matière et Systèmes Complexes, Unité Mixte de Recherche 7057, Centre National de la Recherche Scientifique et Université Paris Diderot—Paris 7, 75205 Paris Cedex 13, France; ^cIstituto Nazionale di Fisica Nucleare (Italy), Sezione di Roma I, Istituto per i Processi Chimico Fisici—Consiglio Nazionale delle Ricerche (Italy), I-00185 Roma, Italy; ^dDipartimento di Fisica, Sapienza Università di Roma, I-00185 Roma, Italy; and ^eLaboratoire de Physique Théorique, Ecole Normale Supérieure, Unité Mixte de Recherche 8549 Centre National de la Recherche Scientifique, 75005, France

Contributed by Giorgio Parisi, September 24, 2012 (sent for review June 12, 2012)

We develop a full microscopic replica field theory of the dynamical transition in glasses. By studying the soft modes that appear at the dynamical temperature, we obtain an effective theory for the critical fluctuations. This analysis leads to several results: we give expressions for the mean field critical exponents, and we analytically study the critical behavior of a set of four-points correlation functions, from which we can extract the dynamical correlation length. Finally, we can obtain a Ginzburg criterion that states the range of validity of our analysis. We compute all these quantities within the hypernetted chain approximation for the Gibbs free energy, and we find results that are consistent with numerical simulations.

mode-coupling theory | perturbative expansion | replica theory

Dynamical heterogeneities in structural glasses have been the object of intensive investigations in the last 15 y (1). The early Adams–Gibbs theory of glass formation was based on the concept of cooperatively rearranging regions with sizes that become larger and larger when the glass region is approached. Such large cooperatively rearranging regions imply the existence of dynamical heterogeneities characterized by a large correlation length. Large-scale dynamical heterogeneities are expected to be present in any framework where glassiness is caused by collective effects: They are, indeed, the smoking guns for these effects (1–4). Therefore, it is not a surprise that two popular approaches to glasses, mode-coupling theory (MCT) (5) and the replica method (6, 7), both agree with the Adams–Gibbs scenario and predict large-scale dynamical heterogeneities with a dynamical correlation length that diverges at the transition to the glass phase. This qualitative prediction is very interesting, but to make additional progresses, it would be important to get quantitative predictions that can be compared with numerical simulations and experiments.

At the mean field level, where both thermodynamic and dynamic aspects can be solved exactly, it is found that the replica and MCT approaches are intimately related. The study of spherical p -spin models, where dynamics are exactly described by a schematic MCT equation and equilibrium displays glassy phenomena related to replica symmetry breaking, shows how the glass transition described by MCT is related to the emergence of metastable states in equilibrium (8, 9). That basic observation, made more than 20 y ago in the work by Kirkpatrick et al. (10), opened the way to the application of the mean field theory of spin glasses to the physics of supercooled liquids and glasses (11–13). Despite this clear relation at the level of mean field schematic models, when one tries to apply the mean field theory to realistic models of simple liquids (5–7, 14, 15), approximations are mandatory, and because of the approximations, the connection between statics and dynamics becomes more difficult to establish. It has been shown in the work by Szamel (16) that, under suitable approximations (similar to the one of MCT), the long time limit of the MCT equations could be derived from a replicated liquid theory. Unfortunately, this time limit leads to expressions that are not variational, and one cannot get an approximation for the free energy from the computation. Using standard liquid theory approximations within replica theory instead (6, 7, 14, 15), one finds strong

discrepancies between predictions from MCT and replicas, which become particularly pronounced in large dimensions (7, 17).

Other than this consistency problem, in finite dimensions, one would like to compute the corrections caused by fluctuations around the mean field approximation. When this program is carried out, one finds that there are two important sources of corrections to the mean field scenario. The first corrections originate from critical fluctuations that become important around the glass transition below the upper critical dimension, like in any standard critical phenomenon (18, 19). The second corrections are nonperturbative phenomena related to activated processes. They can be taken into account by a phenomenological approach, leading to a number of predictions that are in good agreement with experiment (11); however, the theoretical foundations of this approach are still controversial (20), and alternative (but possibly related) phenomenological descriptions of activated relaxation in glasses have been developed, mostly based on the concept of dynamical facilitation (21).

In this paper, we will only consider critical fluctuations around mean field, and therefore, we will not take into account activated processes. Critical fluctuations have been previously described within MCT (18, 22–24). However, field theoretical methods are not yet under complete control in the context of dynamics, and it is, therefore, extremely important to set up a static replica field theoretical description of dynamical heterogeneities in such a way that well-established equilibrium field theory methods, such as the renormalization group, can be applied to the glass transition problem. This result is what we achieve in this paper. We obtain a low-energy effective action that describes critical fluctuations on approaching the glass transition, with coupling constants that are obtained directly from the interparticle interaction potential using standard liquid theory. This process allows us to compute prefactors to the singular behavior of physical observables in the mean field approximation, such as the correlation length or the four-point correlation functions. In addition, we show that an important characterization of dynamics, the MCT exponents, can be obtained within the static replica framework. Using the well-established hypernetted chain approximation (HNC) approximation of liquid theory, we perform explicit computations for hard- and soft-sphere models and Lennard–Jones potentials, and we obtain good agreement with available numerical data. Finally, we introduce a quantitative Ginzburg criterion defining a region, where perturbative corrections to mean field theory can be neglected.

Dynamical Heterogeneities

In this section, we consider a system of N particles in a volume V interacting through a pairwise potential $v(r)$ in a D dimensional space. The dynamical glass transition is characterized by an

Author contributions: S.F., G.P., and F.Z. designed research; S.F., H.J., G.P., P.U., and F.Z. performed research; S.F., H.J., G.P., P.U., and F.Z. contributed new reagents/analytic tools; H.J. and P.U. analyzed data; and S.F., G.P., P.U., and F.Z. wrote the paper.

The authors declare no conflict of interest.

¹To whom correspondence should be addressed. E-mail: giorgio.pari@roma1.infn.it.

This article contains supporting information online at www.pnas.org/lookup/suppl/doi:10.1073/pnas.1216578109/-DCSupplemental.

(apparent) divergence of the relaxation time of density fluctuations, which becomes frozen in the glass phase. If $\hat{\rho}(x, t) = \sum_{i=1}^N \delta(x - x_i(t))$ is the local density at point x and time t and $\rho = \langle \hat{\rho}(x, t) \rangle$ is its equilibrium average, the transition can be conveniently characterized using correlation functions. Consider the density profiles at time 0 and time t , respectively, given by $\hat{\rho}(x, 0)$ and $\hat{\rho}(x, t)$. We can define a local similarity measure of these configurations as (Eq. 1)

$$\hat{C}(r, t) = \int dx f(x) \hat{\rho}\left(r + \frac{x}{2}, t\right) \hat{\rho}\left(r - \frac{x}{2}, 0\right) - \rho^2, \quad [1]$$

where $f(x)$ is an arbitrary smoothing function of the density field with some short-range A . In experiments, $f(x)$ could describe the resolution of the detection system and can be, for instance, a Gaussian of width A .

Let us call $C(t) = V^{-1} \int dr \langle \hat{C}(r, t) \rangle$ the spatially and thermally averaged correlation function. Typically, on approaching the dynamical glass transition T_d , $C(t)$ displays a two-step relaxation, with a fast β -relaxation occurring on shorter times down to a plateau and a much slower α -relaxation from the plateau to zero (5). Close to the plateau at $C(t) = C_d$, one has $C(t) \sim C_d + \mathcal{A}t^{-a}$ in the β -regime. The departure from the plateau (beginning of α -relaxation) is described by $C(t) \sim C_d - Bt^b$. One can define the α -relaxation time by $C(\tau_\alpha) = C(0)/e$. It displays an apparent power-law divergence at the transition, $\tau_\alpha \sim |T - T_d|^{-\gamma}$. All of these behaviors are predicted by MCT (5). In low dimensions, a rapid crossover to a different regime dominated by activation is observed, and the divergence at T_d is avoided; however, the power-law regime is the more robust the higher the dimension (25, 26) or the longer the range of the interaction (27).

It is now well-established, both theoretically and experimentally, that the dynamical slowing is accompanied by growing heterogeneity of the local relaxation in the sense that the local correlations $\hat{C}(r, t)$ display increasingly correlated fluctuations when T_d is approached (1–3, 28). This result can be quantified by introducing the correlation function of $\hat{C}(r, t)$ (i.e., a four-point dynamical correlation) (Eq. 2):

$$G_4(r, t) = \langle \hat{C}(r, t) \hat{C}(0, t) \rangle - \langle \hat{C}(r, t) \rangle \langle \hat{C}(0, t) \rangle. \quad [2]$$

The latter decays, because $G_4(r, t) \sim \exp(-r/\xi(t))$ with a dynamical correlation length that grows at the end of the β -regime and has a maximum $\xi = \xi(t \sim \tau_\alpha)$ that also (apparently) diverges as a power law when T_d is approached.

MCT (5) and its extensions (18, 22–24, 29, 30) give precise predictions for the critical exponents. However, as discussed in the Introduction, this dynamical transition can be also described, at the mean field level, in a static framework. The advantage is that calculations are simplified, and therefore, the theory can be pushed forward, particularly by constructing a reduced field theory and setting up a systematic loop expansion that allows us to obtain detailed predictions for the upper critical dimension and the critical exponents (19). Moreover, very accurate approximations for the static free energy of liquids have been constructed (31), and one can make use of them to obtain quantitative predictions for the physical observables. These predictions are the aim of the rest of this paper.

Connection Between Replicas and Dynamics

In the mean field scenario, the dynamical transition of MCT is related to the emergence of a large number of metastable states, in which the system remains trapped for an infinite time. At long times in the glass phase, the system is able to decorrelate within one metastable state. Hence, we can write (Eq. 3)

$$\langle \hat{C}(r, t \rightarrow \infty) \rangle = \int dx f(x) \overline{\langle \hat{\rho}\left(r + \frac{x}{2}\right) \rangle_m \langle \hat{\rho}\left(r - \frac{x}{2}\right) \rangle_m} - \rho^2, \quad [3]$$

where $\langle \bullet \rangle_m$ denotes an average in a metastable state, and the over line denotes an average over the metastable states with equilibrium weights.

The dynamical transition can be described in a static framework by introducing a replicated version of the system (14, 32): for every particle, we introduce $m - 1$ additional particles identical to the first one. In this way, we obtain m copies of the original system, labeled by $a = 1, \dots, m$. The interaction potential between two particles belonging to replicas a, b is $v_{ab}(r)$. We set $v_{aa}(r) = v(r)$, the original potential, and we fix $v_{ab}(r)$ for $a \neq b$ to be an attractive potential that constrains the replicas to be in the same metastable state. Let us now define our basic fields that describe the one- and two-point density functions (Eq. 4):

$$\begin{aligned} \hat{\rho}_a(x) &= \sum_{i=1}^N \delta(x - x_i^a), \\ \hat{\rho}_{ab}^{(2)}(x, y) &= \hat{\rho}_a(x) \hat{\rho}_b(y) - \hat{\rho}_a(x) \delta_{ab} \delta(x - y). \end{aligned} \quad [4]$$

To detect the dynamical transition, one has to study the two-point correlation functions when $v_{ab}(r) \rightarrow 0$ for $a \neq b$, and in the limit $m \rightarrow 1$, which reproduces the original model (14, 32). In this limit, the two-replica correlation function is, for $a \neq b$ (Eq. 5),

$$\langle \hat{C}_{ab}(r) \rangle = \int dx f(x) \langle \hat{\rho}_a\left(r + \frac{x}{2}\right) \hat{\rho}_b\left(r - \frac{x}{2}\right) \rangle - \rho^2. \quad [5]$$

Because of the limit $v_{ab}(r) \rightarrow 0$, the two replicas fall in the same state but are otherwise uncorrelated inside the state; therefore, we obtain $\langle \hat{C}_{ab}(r) \rangle = \langle \hat{C}(r, t \rightarrow \infty) \rangle$, which provides the crucial identification between replicas and dynamics. Similar mappings can be obtained for four-point correlations.

Replica Field Theory for the Dynamical Transition

We introduce (for convenience) an external field $\nu_a(x)$ that derives from a space-dependent chemical potential, in such a way that the density correlation functions can be obtained by taking the derivative of the free energy with respect to it (31). The free energy is defined as the logarithm of the partition function, and its double Legendre transform defines the Gibbs free energy $\Gamma[\{\rho_a(x)\}, \{\rho_{ab}^{(2)}(x, y)\}]$ (31, 33) (Eq. 6):

$$\begin{aligned} \Gamma &= \frac{1}{2} \sum_{a,b} \int dx dy \left[\rho_{ab}^{(2)}(x, y) \ln \left(\frac{\rho_{ab}^{(2)}(x, y)}{\rho_a(x) \rho_b(y)} \right) \right. \\ &\quad \left. - \rho_{ab}^{(2)}(x, y) + \rho_a(x) \rho_b(y) \right] + \sum_a \int dx \rho_a(x) [\ln \rho_a(x) - 1] \\ &\quad + \sum_{n \geq 3, a_1, \dots, a_n} \frac{(-1)^n}{2^n} \int dx_1 \dots dx_n \rho_{a_1}(x_1) h_{a_1 a_2}(x_1, x_2) \\ &\quad \times \dots \rho_{a_n}(x_n) h_{a_n a_1}(x_n, x_1) + \Gamma_{2PI}, \end{aligned} \quad [6]$$

where $h_{ab}(x, y) = \rho_{ab}^{(2)}(x, y) / \rho_a(x) \rho_b(y) - 1$, and Γ_{2PI} is the sum of two-line irreducible diagrams (33). The average values of the fields in Eq. 4, namely $\bar{\rho}_a(x)$ and $\bar{\rho}_{ab}(x, y)$, can be obtained by solving the saddle point equation (Eq. 7),

$$\frac{\delta \Gamma[\{\rho_a\}, \{\rho_{ab}^{(2)}\}]}{\delta \rho_{ab}^{(2)}(x, y)} \bigg|_{\bar{\rho}_{ab}(x, y)} = \frac{1}{2} v_{ab}(x, y), \quad [7]$$

and similarly, they can be obtained for $\rho_a(x)$. Here, we consider a homogeneous liquid; hence, $\rho_a(x) = \rho$.

We have to assume, at this point, that a mean field approximation of the free energy is available, which we shall use as the starting point of our computations. Within this approximation, we want to study the behavior of $\bar{\rho}_{a\neq b}(x, y)$ in the double limit $m \rightarrow 1$ and $v_{a\neq b} \rightarrow 0$, which signal the dynamical transition: if $T > T_d$, then $\bar{\rho}_{a\neq b}(x, y) = \rho^2$, whereas if $T \leq T_d$, a nontrivial off-diagonal solution persists in the limit $v_{a\neq b} \rightarrow 0$. At the mean field level, the appearance of the nontrivial solution is a bifurcation phenomenon, and therefore, if we come from below the transition and we define $\varepsilon = T_d - T$, we have, for $\varepsilon \rightarrow 0$ (Eq. 8),

$$\bar{\rho}_{a\neq b}(x, y; \varepsilon) = \rho^2 \bar{g}(x - y) + 2\rho^2 \sqrt{\varepsilon} \kappa k_0(x - y), \quad [8]$$

where $k_0(x)$ is normalized as $\int dx k_0(x)^2 = 1$, and κ is a constant. From the saddle point (Eq. 7), we obtain that the Hessian matrix for the off-diagonal elements (i.e., for $a \neq b, c \neq d$) (Eq. 9),

$$M_{ab;cd}(x_1, x_2; x_3, x_4) = \frac{\delta^2 \Gamma[\{\rho_a\}, \{\rho_{ab}^{(2)}\}]}{\delta \rho_{ab}^{(2)}(x_1, x_2) \delta \rho_{cd}^{(2)}(x_3, x_4)}, \quad [9]$$

which is considered as a kernel operator both in standard and replica space, develops a zero mode at T_d . This finding means that, if the transition is approached from below, the fundamental eigenvalue of this operator is proportional to $\sqrt{\varepsilon}$ because of the bifurcation-like phenomenology. Moreover, the eigenvector corresponding to it is $k_0(x - y)$.

Exploiting the replica symmetry of the saddle point solution (Eq. 7), the most general form of the Hessian matrix is given by (Eq. 10)

$$M_{ab;cd}(x_1, x_2; x_3, x_4) = M_1 \left(\frac{\delta_{ac} \delta_{bd} + \delta_{ad} \delta_{bc}}{2} \right) + M_2 \left(\frac{\delta_{ac} + \delta_{ad} + \delta_{bc} + \delta_{bd}}{4} \right) + M_3, \quad [10]$$

where M_1, M_2 , and M_3 depend on x_1, \dots, x_4 . From this equation, one can show that, because the zero mode $k_0(x - y)$ is independent of the replica indices, in the replica limit $m \rightarrow 1$, it is an eigenvector of the kernel operator M_1 . To study the correlation functions for the fields in Eq. 4, we can produce a power series expansion of the Gibbs free energy in terms of the fluctuation of the field $\rho_{a\neq b}^{(2)}(x, y)$ from its saddle point value. Defining the field $\Delta \rho_{ab}(x, y) = \rho_{ab}^{(2)}(x, y) - \bar{\rho}_{ab}(x, y)$, we can expand the Gibbs free energy up to the third order. It is convenient to define p_i and q_i as the momenta conjugated to the half-sum and the difference of the spatial arguments of $\Delta \rho_{ab}(x_i, y_i)$. Using translation invariance, we write the replica action in Fourier space as (Eq. 11)

$$\begin{aligned} \Gamma[\{\Delta \rho_{ab}\}] &= \Gamma[\{\bar{\rho}_{ab}\}] \\ &+ \frac{1}{2} \sum_{a \neq b, c \neq d} \int \frac{dp dq_1 dq_2}{(2\pi)^{3D}} \Delta \rho_{ab}(p, q_1) M_{ab;cd}^{(p)}(q_1, q_2) \Delta \rho_{cd}(-p, q_2) \\ &+ \frac{1}{6} \sum_{ab;cd;ef} \int \frac{dp dp' dq_1 dq_2 dq_3}{(2\pi)^{5D}} L_{ab;cd;ef}(p, p'; q_1, q_2, q_3) \\ &\times \Delta \rho_{ab}(p, q_1) \Delta \rho_{cd}(p', q_2) \Delta \rho_{ef}(-p - p', q_3). \end{aligned} \quad [11]$$

Because of the zero mode of the Hessian matrix, the connected correlation function of $\Delta \rho_{ab}(x, y)$ shows critical fluctuations at the transition.

To make the connection with the dynamical correlation, we define an overlap function among replicas, $q_{ab}(r)$, as in Eq. 1, substituting the configurations at time 0 and t by replicas a and b . We expect that all of the critical fluctuations of $q_{ab}(r)$ can be captured by a projection on the zero mode, leading from Eq. 11 to an effective action. We can study the fluctuations of $q_{ab}(r)$ for generic functions f by performing a Legendre transform of Eq. 11. However, the results are quite involved, and here, for clarity, we will first consider the simplest case, where $f(x) = k_0(x)$. Of course, this process is not a practical choice for numerical simulations or experiments, because k_0 is quite difficult to measure; however, the theoretical computations are much simpler in this case. Later, we will show that any other choice of f leads to the same results for the critical quantities, and it only affects the prefactor of the correlation functions. The projection onto the zero mode can be done by choosing $\Delta \rho_{ab}(x, y) = k_0(x - y) \phi_{ab}(\frac{x+y}{2})$ and substituting this finding in Eq. 11. The field $\phi_{ab}(x)$ is the component of the overlap along the zero mode, and we perform a perturbative expansion at small momentum p . The effective replica field theory that arises is equivalent to a Landau-like gradient expansion along the critical modes (Eq. 12):

$$\begin{aligned} \Gamma[\{\phi_{ab}\}] &= \frac{1}{2} \int dp \left(\sum_{a \neq b} (\mu \sqrt{\varepsilon} + \sigma p^2) |\phi_{ab}(p)|^2 \right. \\ &+ m_2 \sum_a \left| \sum_b \phi_{ab}(p) \right|^2 + m_3 \left| \sum_{a \neq b} \phi_{ab}(p) \right|^2 \Big) \\ &+ \frac{w_1}{6} \int \sum_{a \neq b \neq c \neq a} \frac{dp dp'}{(2\pi)^{2D}} \phi_{ab}(p) \phi_{bc}(p') \phi_{ca}(-p - p') \\ &+ \frac{w_2}{6} \int \sum_{a \neq b} \frac{dp dp'}{(2\pi)^{2D}} \phi_{ab}(p) \phi_{ab}(p') \phi_{ab}(-p - p'). \end{aligned} \quad [12]$$

Eq. 12 is the effective low-energy replica field theory that we will use to compute the critical properties of the system. All of its coefficients can, in principle, be computed from the microscopic details of the systems after an approximation for Γ is available. In fact, they can be given explicit expressions as functions of derivatives of the Gibbs free energy and the zero mode, which both derive from the interaction potential (SI Text).

Correlation Functions, Correlation Length, and Critical Exponents

The effective replica field theory in Eq. 12 can be used to compute the MCT parameter λ . This quantity is related to the MCT critical exponents that control the approach to the plateau by the relation (Eq. 13)

$$\lambda = \frac{\Gamma(1-a)^2}{\Gamma(1-2a)} = \frac{\Gamma(1+b)^2}{\Gamma(1+2b)}. \quad [13]$$

In addition, the exponent that controls the growth of the relaxation time $\tau_\alpha \sim |T - T_d|^{-\gamma}$ is given by $\gamma = 1/(2a) + 1/(2b)$. Although λ is a dynamical parameter, it has been explicitly shown recently in disordered mean field models, and it can be argued on general ground (34) that this parameter can be related to a ratio of six-point static correlation functions computable in the replica field theory that we have just derived. In this scheme, the exponent parameter is given by (Eq. 14)

$$\lambda = \frac{w_2}{w_1}. \quad [14]$$

Moreover, the field theory above can be used at the Gaussian level to obtain the correlation functions of the overlap. The

analysis of the quadratic part of Eq. 12 shows that the correlation length is controlled by the diagonal part, being m_2 and m_3 finite at the transition. The result is (Eq. 15)

$$\xi = \xi_0 \epsilon^{-1/4}, \quad \xi_0 = \sqrt{\frac{\sigma}{\mu}}, \quad [15]$$

and it corresponds to the divergence of the dynamical correlation length $\xi(t)$ in the β -regime (22–24).

Moreover, we can compute in detail the critical behavior of many possible dynamical four-point functions that are identified with different matrix elements of the inverse of the Hessian matrix in Eq. 9 (19). Here, we give the results for the simplest one, the so-called in-state or thermal susceptibility, which is given by (Eq. 16)

$$G_{\text{th}}(r, t) = \mathbf{E}_0 \left[\langle \hat{C}(r, t) \hat{C}(0, t) \rangle - \langle \hat{C}(r, t) \rangle \langle \hat{C}(0, t) \rangle \right], \quad [16]$$

where $\mathbf{E}_0[\cdot]$ has to be intended as the average over the initial positions of the particles, whereas $\langle \bullet \rangle$ is an average over different trajectories (i.e., over the noise for Langevin dynamics or over the initial velocities for Newton dynamics). In the long time limit, this quantity is one of the critical contributions to the $G_4(r, t)$ in Eq. 2, and it can be computed directly from the replica field theory above (19). Here, we had to generalize the calculation in ref. 19 to take into account the structure of the zero mode and the presence of the smoothing function $f(x)$. The result is (Eq. 17)

$$G_{\text{th}}(p) = \frac{G_0 \epsilon^{-1/2}}{1 + \xi^2 p^2}, \quad G_0 = \frac{1}{\mu} \int \frac{dq}{(2\pi)^D} f(-q) k_0(q). \quad [17]$$

We obtain that the correlation length and its prefactor are not dependent on the function $f(x)$ and are always given by Eq. 15. The only dependence on $f(x)$ of the four-point function is in the prefactor G_0 . The full four-point correlation (Eq. 2) is known to display a doubled singularity with respect to Eq. 17. In fact, with the choice $f(x) = k_0(x)$, one finds $G_4(p) = G_{\text{th}}(p) - (m_2 + m_3) G_{\text{th}}(p)^2$ (19). For generic $f(x)$, the computation of the prefactor is more involved and will not be presented here.

A Ginzburg Criterion

All of the calculations above are based on the assumption that a mean field approximation of the free energy of the system is given. From these calculations, we derive the effective Landau field theory (Eq. 12). From its coefficients, we extracted all of the mean field critical exponents as well as microscopic expressions for the prefactors. Now, we can check whether loop corrections to the effective field theory strongly affect the mean field predictions by means of a Landau–Ginzburg computation. In other words, we want to see whether the loop corrections to the bare correlation function are small. In principle, we should take the field theory derived above, and then, we should compute the first nontrivial loop diagrams that give the first correction to the propagator in replica space. This computation is quite involved, because we have to deal with replica indices. However, it has been shown in ref. 19 that the leading divergent behavior of the above field theory can be mapped to the one of a scalar field in a cubic potential with a random field (Eq. 18):

$$S(\phi) = \frac{1}{2} \int dx \phi(x) (-\sigma \nabla^2 + \mu \sqrt{\epsilon} + \delta m(g, \Delta)) \phi(x) + \frac{g}{6} \int dx \phi^3(x) + \int dx (h_0(x) + \delta h(g, \Delta)) \phi(x), \quad [18]$$

where the random field has zero mean and correlation $\overline{h_0(x)h_0(y)} = \Delta \delta(x - y)$, and the coupling constants are given by $g = w_2 - w_1$ and $\Delta = -m_2 - m_3$.

The terms $\delta m(g, \Delta)$ and $\delta h(g, \Delta)$ are counterterms needed to enforce that the critical point is not shifted by loop corrections. By computing the first one-loop diagram and imposing that the relative correction is small with respect to the bare quantity, we arrive to the following Landau–Ginzburg criterion (19)

$$1 \gg \text{Gi} \xi^{8-D}, \quad [19]$$

where the (dimensional) Ginzburg number is given by (Eq. 20)

$$\text{Gi} = \frac{g^2 \Delta}{4(4\pi)^{D/2}} \Gamma\left(4 - \frac{D}{2}\right). \quad [20]$$

This computation is correct only below the upper critical dimension $D_u = 8$. For $D \geq D_u$, the theory is divergent in the UV, and the Ginzburg number depends on the microscopic details; however, the critical exponents coincide with the mean field ones.

Results in the HNC Approximation

Up to now, the calculations were very general, and the results above hold for any given approximation of the replicated free energy functional that displays the correct mean field glassy phenomenology. One of the advantages of our static approach is, indeed, that it can be systematically improved by considering more accurate approximations of Γ .

Here, we report results obtained from the replicated HNC approach that amount to neglecting the $\Gamma_{2\text{PI}}$ term in Eq. 6, which has been shown to give the correct glassy phenomenology at the mean field level (14, 15). Applying the formulae above, we find that, in the HNC approximation, the parameter λ is given by (Eq. 21)

$$\lambda = \frac{\frac{1}{\rho^4} \int dx \frac{k_0^3(x)}{g^2(x)}}{\frac{1}{\rho^3} \int \frac{dq}{(2\pi)^D} k_0^3(q) [1 - \rho \Delta c(q)]^3}, \quad [21]$$

where $\tilde{g}(x) = \overline{\rho_{a \neq b}}(x)/\rho^2$, $\Delta c(q) = c_{aa}(q) - c_{a \neq b}(q)$, and the direct correlation function $c_{ab}(q)$ is related to $h_{ab}(q)$ by the replicated Ornstein–Zernike relation (14). Similar expressions can be obtained for all of the other coefficients (SI Text).

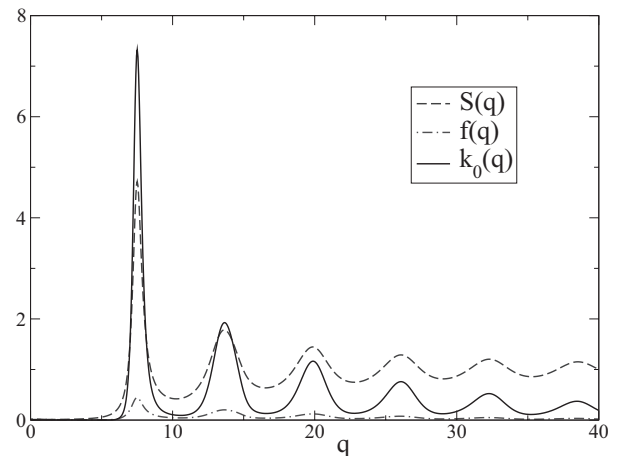


Fig. 1. The zero mode $k_0(q)$, the structure factor $S(q)$, and the nonergodicity factor $f(q)$ for HS at the dynamical transition $\rho_d = 1.176$ in the HNC approximation.

Table 1. Numerical values of the coefficients of the effective action and the physical quantities from the HNC approximation

System	T	ρ_d	w_1	w_2	m_2	m_3	σ	μ	λ	ξ_0	G_0	Gi
SS-6	1	6.691	0.121	0.0845	-0.229	0.0273	0.0484	0.130	0.697	0.601	224	0.370
SS-9	1	2.912	2.41	1.70	-1.34	0.157	0.405	1.35	0.705	0.548	34.3	0.166
SS-12	1	2.057	8.58	6.08	-2.89	0.328	0.938	3.77	0.709	0.498	14.2	0.154
LJ	0.7	1.407	33.1	23.5	-6.39	0.719	2.45	10.3	0.709	0.489	6.00	0.108
HarmS	10^{-3}	1.335	40.4	29.1	-8.34	0.850	1.92	19.3	0.719	0.315	2.82	0.535
HarmS	10^{-4}	1.196	51.5	38.9	-10.0	0.957	2.03	27.0	0.756	0.274	1.69	0.622
HarmS	10^{-5}	1.170	54.3	41.5	-10.3	0.979	2.09	27.1	0.764	0.278	1.66	0.593
HS		1.169	54.5	41.5	-10.3	0.984	2.10	26.7	0.761	0.280	1.67	0.606

For each potential, lengths are given in units of r_0 , and energies are given in units of ε , with $k_B = 1$. Data are at fixed temperature using density as a control parameter with $\varepsilon = \rho_d - \rho$.

To produce concrete numerical results, we have numerically solved the HNC equations by standard methods (14) for a large variety of systems in $D = 3$. In particular, we have considered

Hard Spheres (HS): $v(r) = 0$ for $r > r_0$ and $v(r) = \infty$ otherwise.

Harmonic Spheres (HarmS): $v(r) = \varepsilon(r_0 - r)^2 \theta(r_0 - r)$.

Soft Spheres (SS- n): $v(r) = \varepsilon(r_0/r)^n$, with $n = 6, 9, 12$.

Lennard-Jones (LJ): $v(r) = 4\varepsilon[(r_0/r)^{12} - (r_0/r)^6]$.

Weeks-Chandler-Andersen (WCA): $v(r) = 4\varepsilon[(r_0/r)^{12} - (r_0/r)^6 + 1/4]\theta(r_0 2^{1/6} - r)$.

In all cases, we fix units in such a way that $r_0 = 1$, $\varepsilon = 1$, and the Boltzmann constant $k_B = 1$. For HS and SS, temperature is irrelevant (for SS, the only relevant parameter is a combination of density and temperature; hence, we fix $T = 1$ for convenience), and we study the system as a function of density to determine the glass transition density ρ_d . For the other systems, we studied the transition as a function of both density and temperature.

To obtain numerically the zero mode, we have used the definition in Eq. 8 and estimated it by the numerical derivative of $\bar{g}(r)$ with respect to $\sqrt{\varepsilon}$ when $\varepsilon \rightarrow 0$. A plot of the zero mode for HS is in Fig. 1. Interestingly, we find that the zero mode has the same structure in Fourier space as the static structure factor $S(q)$ and the nonergodicity parameter $f(q)$, which is the Fourier transform of the long time limit of Eq. 1 in the glass phase (5). This finding offers a rationalization of the common practice of concentrating on momenta of the order of the peak of $S(q)$ in the study of glassy relaxation.

From the zero mode, we can compute all of the coefficients of the effective action from which we obtain the physical quantities. In particular, we can compute the prefactor ξ_0 of the growth of the correlation length and the Ginzburg number. Moreover, we have computed the prefactor G_0 of the in-state susceptibility (Eq. 17) using a box function $f(x) = (2A)^{-D/2} \prod_{\alpha=1}^D \theta(A^2 - x_\alpha^2)$, where $\theta(x)$ is the Heaviside step function and $A = 0.1r_0$. All of the results are collected in Tables 1 and 2.

The value of λ that we find is almost the same for all investigated systems and is consistent with the result of MCT (5) and numerical results for these systems. Note, however, that the location of the critical point predicted by HNC is different from the one of MCT

(e.g., for HS, HNC predicts $\rho_d = 1.169$, whereas MCT predicts $\rho_d = 0.978$) (5). This result is an example of the fact, already mentioned in the Introduction, that different approximation schemes lead to different results. Another example of this problem is obtained by comparing the results for LJ and WCA at $\rho = 1.2, 1.4$ (Table 2) with MCT and the numerical data reported in table 1 in ref. 35. The most interesting numerical result is the Ginzburg number. We predict that (perturbative) corrections to mean field results in $D = 3$ should remain small as long as the dynamical correlation length is smaller than ~ 1 . Note that a different Ginzburg criterion for the validity of MCT, based on a phenomenological approach, has been derived in ref. 20: the results of that analysis also suggest that corrections to mean field will appear when the correlation length is ~ 1 .

Unfortunately, not many data for the critical behavior of four-point correlations in the β -regime are available (36, 37). It would, thus, be very interesting to get high-precision simulation data in the β -regime.

Conclusions

We have studied the replica field theory for the dynamical transition in glasses in detail. By using the HNC approximation, we have computed many physical observables directly from the microscopic expression of the interaction potential. First, we provided a way to compute the mode-coupling exponent parameter λ . The numerical values obtained are in good agreement with the experimental and numerical estimates. Second, we have computed the prefactor of the correlation length at the transition together with the prefactor of the in-state four-point correlation function. Third, we have self-consistently closed our analysis by looking at the loop corrections to the mean field quantities to produce a Ginzburg criterion that states how close we have to be to the dynamical transition to see deviations from mean field theory. We found that the range currently accessible to numerical simulations in 3D is close to the point where such corrections should become important. Of course, nonperturbative corrections (activated processes) are not included in our analysis, but they are responsible for strong deviations from the MCT regimen when the transition is approached.

Our analysis is quite general, because it relies only on the assumption that the approximation scheme used for the Gibbs free energy shows the correct mean field glassy phenomenology.

Table 2. Same as Table 1, but here, the data are at fixed density using temperature as a control parameter with $\varepsilon = T_d - T$

System	ρ	T_d	w_1	w_2	m_2	m_3	σ	μ	λ	ξ_0	G_0	Gi
LJ	1.2	0.335	58.2	41.4	-8.94	0.999	3.65	14.2	0.711	0.507	4.56	0.0937
LJ	1.27	0.438	47.9	33.8	-7.96	0.916	3.18	11.1	0.705	0.536	5.74	0.102
LJ	1.4	0.683	33.7	23.9	-6.46	0.726	2.49	7.24	0.710	0.586	8.52	0.106
WCA	1.2	0.325	61.0	42.9	-9.65	1.05	3.29	15.1	0.703	0.467	4.37	0.179
WCA	1.4	0.692	34.5	24.2	-6.68	0.746	2.39	7.21	0.701	0.576	8.67	0.143

Hence, it can, in principle, be repeated in different approximation schemes to go beyond HNC and obtain more accurate expressions for physical quantities.

ACKNOWLEDGMENTS. The PhD work of H.J. is funded by a Foundation Fondation Capital Fund Management-Jean Pierre Aguilar grant. The European Research Council has provided financial support through European Research Council Grant 247328.

1. Berthier L, Biroli G, Bouchaud JP, Cipelletti L, van Saarloos W, eds (2011) *Dynamical Heterogeneities and Glasses* (Oxford Univ Press, London).
2. Franz S, Parisi G (2000) On non-linear susceptibility in supercooled liquids. *J Phys Condens Matter* 12:6335.
3. Berthier L, et al. (2005) Direct experimental evidence of a growing length scale accompanying the glass transition. *Science* 310(5755):1797–1800.
4. Montanari A, Semerjian G (2006) Rigorous inequalities between length and time scales in glassy systems. *J Stat Phys* 125:23–54.
5. Götze W (2009) *Complex Dynamics of Glass-Forming Liquids: A Mode-Coupling Theory* (Oxford Univ Press, New York), Vol 143.
6. Mezard M, Parisi G (2012) *Glasses and Replicas*, eds Wolynes PG, Lubchenko V (Wiley, New York).
7. Parisi G, Zamponi F (2010) Mean-field theory of hard sphere glasses and jamming. *Rev Mod Phys* 82:789–845.
8. Cugliandolo LF, Kurchan J (1993) Analytical solution of the off-equilibrium dynamics of a long-range spin-glass model. *Phys Rev Lett* 71(1):173–176.
9. Castellani T, Cavagna A (2005) Spin glass theory for pedestrians. *J Stat Mech* 2005: P05012.
10. Kirkpatrick TR, Thirumalai D, Wolynes PG (1989) Scaling concepts for the dynamics of viscous liquids near an ideal glassy state. *Phys Rev A* 40(2):1045–1054.
11. Lubchenko V, Wolynes PG (2007) Theory of structural glasses and supercooled liquids. *Annu Rev Phys Chem* 58:235–266.
12. Cavagna A (2009) Supercooled liquids for pedestrians. *Phys Rep* 476:51–124.
13. Berthier L, Biroli G (2011) Theoretical perspective on the glass transition and amorphous materials. *Rev Mod Phys* 83:587–645.
14. Mézard M, Parisi G (1996) A tentative replica study of the glass transition. *J Phys A Math Gen* 29:6515.
15. Cardenas M, Franz S, Parisi G (1998) Glass transition and effective potential in the hypernetted chain approximation. *J Phys A Math Gen* 31:L163–L169.
16. Szamel G (2010) Dynamic glass transition: Bridging the gap between mode-coupling theory and the replica approach. *EPL* 91:56004.
17. Charbonneau P, Ikeda A, Parisi G, Zamponi F (2011) Glass transition and random close packing above three dimensions. *Phys Rev Lett* 107(18):185702.
18. Biroli G, Bouchaud J (2007) Critical fluctuations and breakdown of the Stokes-Einstein relation in the mode-coupling theory of glasses. *J Phys Condens Matter* 19:205101.
19. Franz S, Parisi G, Ricci-Tersenghi F, Rizzo T (2011) Field theory of fluctuations in glasses. *Eur Phys J E Soft Matter* 34:1–17.
20. Biroli G, Bouchaud J (2012) *The Random First-Order Transition Theory of Glasses: A Critical Assessment*, eds Wolynes PG, Lubchenko V (Wiley, New York).
21. Keys AS, Hedges LO, Garrahan JP, Glotzer SC, Chandler D (2011) Excitations are localized and relaxation is hierarchical in glass-forming liquids. *Phys Rev X* 1:021013.
22. Biroli G, Bouchaud JP, Miyazaki K, Reichman DR (2006) Inhomogeneous mode-coupling theory and growing dynamic length in supercooled liquids. *Phys Rev Lett* 97(19):195701.
23. Berthier L, et al. (2007) Spontaneous and induced dynamic fluctuations in glass formers. I. General results and dependence on ensemble and dynamics. *J Chem Phys* 126(18):184503.
24. Berthier L, et al. (2007) Spontaneous and induced dynamic correlations in glass formers. II. Model calculations and comparison to numerical simulations. *J Chem Phys* 126(18):184504.
25. Charbonneau P, Ikeda A, van Meel JA, Miyazaki K (2010) Numerical and theoretical study of a monodisperse hard-sphere glass former. *Phys Rev E Stat Nonlin Soft Matter Phys* 81(4 Pt 1):040501.
26. Charbonneau P, Ikeda A, Parisi G, Zamponi F (2012) Dimensional study of the caging order parameter at the glass transition. *Proc Natl Acad Sci USA* 109(35):13939–13934.
27. Ikeda A, Miyazaki K (2011) Glass transition of the monodisperse Gaussian core model. *Phys Rev Lett* 106(1):015701.
28. Donati C, Franz S, Glotzer S, Parisi G (2002) Theory of non-linear susceptibility and correlation length in glasses and liquids. *J Non Cryst Solids* 307:215–224.
29. Szamel G (2008) Divergent four-point dynamic density correlation function of a glassy suspension. *Phys Rev Lett* 101(20):205701.
30. Szamel G, Flenner E (2010) Diverging length scale of the inhomogeneous mode-coupling theory: A numerical investigation. *Phys Rev E Stat Nonlin Soft Matter Phys* 81(3 Pt 1):031507.
31. Hansen JP, McDonald IR (1986) *Theory of Simple Liquids* (Academic, London).
32. Monasson R (1995) Structural glass transition and the entropy of the metastable states. *Phys Rev Lett* 75(15):2847–2850.
33. Morita T, Hiroike K (1961) A new approach to the theory of classical fluids. III. *Prog Theor Phys* 25:537.
34. Caltagirone F, et al. (2012) Critical slowing down exponents of mode coupling theory. *Phys Rev Lett* 108(8):085702.
35. Berthier L, Tarjus G (2010) Critical test of the mode-coupling theory of the glass transition. *Phys Rev E Stat Nonlin Soft Matter Phys* 82(3 Pt 1):031502.
36. Stein RSL, Andersen HC (2008) Scaling analysis of dynamic heterogeneity in a supercooled Lennard-Jones liquid. *Phys Rev Lett* 101(26):267802.
37. Karmakar S, Dasgupta C, Sastry S (2010) Comment on “Scaling analysis of dynamic heterogeneity in a supercooled Lennard-Jones liquid”. *Phys Rev Lett* 105(1):019801.

Supporting Information

Supporting Information Corrected June 13, 2013

Franz et al. 10.1073/pnas.1216578109

SI Text

This text is organized in three parts. In the first part, we give a sketch of the line of reasoning that leads to the effective action used to describe the dynamical transition, and we give all of the expressions for the coefficients of the same action in terms of the interparticle potential. We use a generic framework without specifying the approximation used to compute the Gibbs free energy, and then, we give the expressions in the hypernetted chain approximation (HNC) case. The second part is devoted to the Ginzburg criterion: we describe the guidelines of the computation by showing which diagrams have been taken into account to produce the first correction to the bare four-point function that has been given in the text. The third section contains some details on the numerical calculations, and it is useful just to understand how our results can be improved numerically.

Coefficients of the Replica Gibbs Free Energy. As in the text, we assume that the glassy phenomenology manifests itself in the singular behavior of the off-diagonal field $\rho_{a \neq b}(x, y)$ that has a diverging derivative with respect to temperature when the critical point is approached. This finding implies that the Hessian (or mass) kernel operator develops a zero mode. Actually, we remember here that, because of the replica symmetry of the saddle point, only one (i.e., M_1) of the three kernel operators M_1 , M_2 , and M_3 has a zero mode. This result implies that the field $\rho^{(2)}$ can be decomposed on the eigenvectors of M_1 . Because we want to give the expressions for the diverging part of the correlation function, we can simply disregard the excited modes that are finite and take into account only the projection of the dynamical field $\rho^{(2)}$ on the zero mode. Practically, this process is the same as putting to infinity the masses relative to the projections of the dynamical field on the excited states of the kernel operator M_1 . By using this process, we can produce a gradient expansion for the replicated Gibbs free energy. The simplest way is to impose that the fluctuations of the dynamical field from the saddle point solution are proportional to the zero mode (Eq. S1):

$$\Delta \rho_{ab}(x, y) = \phi_{ab} \left(\frac{x+y}{2} \right) k_0(x-y). \quad [\text{S1}]$$

Therefore, the expressions for the coefficients of the effective action for the critical fluctuations can be computed straightforwardly. Let us consider first the expression for σ and μ . They come along in this way. The kernel operator M_1 has a ground-state eigenvalue $\lambda_0(p) = \mu\sqrt{\epsilon} + \sigma p^2 + O(p^4)$. For small momentum (which means that we look at the correlation of two fluctuations of the dynamical field that is at a very large distance), the expressions for μ and σ can be computed using perturbation theory for the eigenvalue problem for the kernel M_1 , where the small perturbative parameter is exactly the momentum p . The final expressions are given by (Eq. S2)

$$\mu = \lim_{\epsilon \rightarrow 0} \frac{d}{d\sqrt{\epsilon}} \int \frac{d^D q d^D k}{(2\pi)^{2D}} k_0(q) M_1^{(p=0)}(q, k) k_0(q) \quad [\text{S2}]$$

and (Eq. S3)

$$\sigma = \lim_{\epsilon \rightarrow 0} \int \frac{d^D q d^D k}{(2\pi)^{2D}} k_0(q) \frac{\partial}{\partial p^2} M_1^{(p)}(q, k) \Big|_{p=0} k_0(q), \quad [\text{S3}]$$

where the zero mode is supposed to be normalized. In the same spirit, the two other masses m_i , $i = 2, 3$, are given by (Eq. S4)

$$m_i = \lim_{\epsilon \rightarrow 0} \int \frac{d^D q d^D k}{(2\pi)^{2D}} k_0(q) M_i^{(p=0)}(q, k) k_0(q). \quad [\text{S4}]$$

At this point, it is clear how the expressions for the two cubic coefficients w_1 and w_2 can be obtained, defining (Eq. S5)

$$L_{ab;cd;ef}(x_1, \dots, x_6) = \frac{\delta^3 \Gamma[\rho, \rho^{(2)}]}{\delta \rho_{ab}^{(2)}(x_1, x_2) \delta \rho_{cd}^{(2)}(x_3, x_4) \delta \rho_{ef}^{(2)}(x_5, x_6)}. \quad [\text{S5}]$$

Then, they are given by the following equations (Eq. S6):

$$w_{1,2} = \int d^D x_1, \dots, d^D x_6 k_0(x_1 - x_2) \dots k_0(x_5 - x_6) W_{1,2}, \quad [\text{S6}]$$

where (Eq. S7)

$$W_1 = L_{ab,bc,ca} - 3L_{ab,ac,bd} + 3L_{ac,bc,de} - L_{ab,cd,ef} \quad [\text{S7}]$$

and (Eq. S8)

$$W_2 = \frac{1}{2} L_{ab,ab,ab} - 3L_{ab,ab,ac} + \frac{3}{2} L_{ab,ab,cd} + 3L_{ab,ac,bd} + 2L_{ab,ac,ad} - 6L_{ac,bc,de} + 2L_{ab,cd,ef}. \quad [\text{S8}]$$

From the expressions for w_1 and w_2 , we can extract the general expression for the exponent parameter λ . However, all of the calculations above rely on the assumption that the replicated Gibbs free energy can be computed exactly. This result is not possible in the general case, and, as we have said in the text, we have to recast in some given mean field-like approximation that has the correct glassy phenomenology. Here, we will give all of the expressions above in the HNC approximation, where the derivatives of the Gibbs free energy can be computed exactly. The expressions for σ and μ are (Eq. S9)

$$\begin{aligned} \mu &= \frac{2\kappa}{\rho} \int \frac{d^D q}{(2\pi)^D} k_0^3(q) [1 - \rho \Delta c(q)] - \kappa \int d^D x \frac{k_0^3(x)}{\rho^2 g^2(x)} \\ \sigma &= \frac{1}{8\rho} \int \frac{d^D q}{(2\pi)^D} k_0^2(q) [\rho \Delta c(q) - 1] \\ &\quad \times \left[\left(\Delta c''(q) - \frac{\Delta c'(q)}{q} \right) \cos^2 \theta + \frac{\Delta c'(q)}{q} \right] \\ &\quad - \frac{1}{8} \int \frac{d^D q}{(2\pi)^D} k_0^2(q) (\Delta c'(q))^2 \cos^2 \theta, \end{aligned} \quad [\text{S9}]$$

where $\Delta c(q) = c(q) - \tilde{c}(q)$ is the difference between the diagonal and off-diagonal part of the matrix of the direct correlation functions defined through the Ornstein Zernike equation, and θ is the polar angle in D -dimensional polar coordinates. The expressions for the other two mass terms are given by (Eq. S10)

$$m_2 = - \int \frac{d^D q}{(2\pi)^D} k_0^2(q) \tilde{c}(q) \left[\frac{1}{\rho} - \Delta c(q) \right]$$

$$m_3 = \frac{1}{2} \int \frac{d^D q}{(2\pi)^D} k_0^2(q) \tilde{c}^2(q). \quad [\text{S10}]$$

By computing the third derivative of the replicated Gibbs free energy in the HNC approximation, we get the expression for w_1 and w_2 (Eq. S11):

$$w_1 = - \frac{1}{8\rho^3} \int \frac{d^D q}{(2\pi)^D} k_0^3(q) \tilde{c}(q) [1 - \rho \Delta c(q)]^3$$

$$w_2 = - \frac{1}{16\rho^4} \int d^D x \frac{k_0^3(x)}{\tilde{g}^2(x)}. \quad [\text{S11}]$$

Ginzburg Criterion. In this section, we give a guideline for the computation of the Ginzburg criterion. In the text, we have said that, at the dynamical point where the number of replicas goes to one, the leading behavior of the correlation functions of the two-points function $\rho^{(2)}$ can be computed using a field theory for a scalar quantity described by a cubic potential in a random field. This observation simplifies a lot of the loop expansion, because it does not involve replica indices that complicate the perturbative analysis. With reference to the action defined in Eq. 18 in the text, we can give a perturbative expression for the two-point function of the field $\phi(x)$. The bare propagator is given as usual by $G_0^{-1}(p) = \sigma p^2 + \mu\sqrt{\epsilon} + \delta m$. To obtain the two-point function, it is quite useful to write down the generating functional of the correlation functions $W[J] = \ln Z[J]$, where we can put $J(x) = h_0(x) + \delta h$, and h_0 is an external field that can be used to extract the correlation function by taking the derivative with respect to it. Introducing the following diagrammatic notation (Eq. S12)

$$J(x) = \circ \quad h_0(x) = \bullet \quad \delta h(g, \Delta) = \bullet, \quad [\text{S12}]$$

we have that (Eq. S13)

$$\overline{\langle \phi(x) \rangle} = \text{diagram with red dot} + \text{diagram with blue dot and loop} + \text{diagram with loop} . \quad [\text{S13}]$$

We impose that the critical point is not shifted by the perturbative terms; therefore, we also want $\overline{\langle \phi(x) \rangle} = 0$, from which we see that the counterterm δh is of order g . Now let us look at the one-loop correction to the propagator. Using

the fact that the expectation value of ϕ is zero, we obtain

$$\overline{\langle \phi(x) \phi(y) \rangle} = G_0(x-y) + \text{diagram with blue dot and loop} + \text{diagram with loop} + \dots$$

We are interested in the most infrared divergent diagrams (in the limit where $T \rightarrow T_d$). This interest means that we can neglect the second diagram, and we can consider only the first one (which is exactly what happens in the perturbative expansion of the Random Field Ising Model). The inverse of the renormalized susceptibility reads (Eq. S14)

$$m_R^2 = G^{-1}(p=0) = m_0^2 + \delta m - \frac{\Delta g^2}{2(2\pi)^D} \int^\Lambda d^D q \frac{1}{(\sigma q^2 + m_0^2)^3}, \quad [\text{S14}]$$

where $m_0^2 = \mu\sqrt{\epsilon}$. By taking the derivative with respect to m_0^2 , we obtain (Eq. S15)

$$\frac{dm_R^2}{dm_0^2} = 1 + 3 \frac{\Delta g^2}{2(2\pi)^D} \int^\Lambda d^D q \frac{1}{(\sigma q^2 + m_0^2)^4}. \quad [\text{S15}]$$

By imposing that the second term on the right side is smaller than one and computing the loop integral, we get the expression 19 and Eq. 20 in the text.

Details on the Numerics. To produce the numerical values collected in the tables, we have solved numerically the HNC equations in 3D. This solving is a quite easy task, because such equations can be solved by an iterative Picard scheme. However, the solution requires the use of Fourier transforms. Working in spherical coordinates thanks to the rotational invariance of the system, we have two natural cutoffs. The first one fixes the maximal distance L (infrared cutoff); hence, we only keep $g(r)$ for $0 \leq r \leq L$. The other one is related to the precision with which we measure the position of the particles (UV cutoff): the possible values of r are discretized in such a way that, in the unit interval, there are N equispaced possible positions; therefore, the precision is $1/N$. The data presented in the tables are relative to the larger cutoffs that we have. In particular, the infrared cutoff is fixed to $L = 16$, where the unit distance is the diameter of the particles or the interaction range of the potential. The UV cutoff is fixed at $n = 256$. A remark must be made on the way that we computed the critical point and the zero mode. In fact, to observe the correct $\sqrt{\epsilon}$ behavior of the off-diagonal solution, we need to be quite close to the critical point, because otherwise, this behavior is hidden by the subleading ϵ behavior. To give a precise estimate of the critical point, we have collected a sequence of solutions of the HNC equation varying the temperature or the density, depending on the case under study, and we have fitted these data with a $\sqrt{\epsilon}$ behavior. After we have identified the critical point, we have computed the zero mode using the definition given by Eq. 8 in the text directly.